One-dimensional laser cooling below the Doppler limit

V. Finkelstein, P.R. Berman, and J. Guo
Department of Physics, New York University, 4 Washington Place, New York, New York 10003
(Received 23 July 1991)

A theoretical analysis is given for one-dimensional laser cooling below the Doppler limit of $J = \frac{1}{2}$ ground-state atoms. The laser field consists of a pair of counterpropagating, linearly polarized, low-power beams, whose polarization directions differ by an angle θ ($0 \leq \theta \leq \pi/2$). For $\theta \ll 1$, the effective optical-pumping time is shown to increase strongly near the nodes of the standing wave, and the cooling force can be much larger than that for $\theta = \pi/2$. Moreover, for $\theta \ll 1$, it can be shown that the stimulated part of the atomic diffusion is reduced considerably as compared with that for $\theta = \pi/2$. As a consequence it is possible to achieve an equilibrium atomic distribution that, for $\theta \ll 1$, is characterized by a mean kinetic energy that is lower than that predicted to occur for $\theta = \pi/2$. The equilibrium velocity distribution is not necessarily Maxwellian, and thus the temperature of the atomic ensemble may not be well defined. The achievable kinetic energy is so small that the cooled atoms may be trapped in the vicinity of the laser-field nodes.

PACS number(s): 42.50.Vk, 32.80.Pj

I. INTRODUCTION

In the past several years it has been demonstrated both experimentally and theoretically that the laser cooling of neutral atoms can lead to an equilibrium atomic kinetic energy E_k much smaller than that given by the Doppler limit for two-level atoms, that is $E_k \ll \hbar\Gamma$, where Γ is the spontaneous decay rate of an excited atomic state. It has been shown that the sub-Doppler-limit laser cooling is directly related to effects arising from the multilevel structure of the atomic ground state (Refs. [1–7]). Efficient sub-Doppler-limit cooling is obtained using a very weak laser field satisfying

$$f^2 \ll \delta^2 + \Gamma^2, \tag{1.1}$$

where $f = E\mu/\hbar$ is the Rabi frequency, and μ the dipole moment of the atomic transition. The laser field has an amplitude E and a frequency ω_L detuned from the atomic resonant frequency ω_A by an amount δ given by

$$\delta = \omega_L - \omega_A. \tag{1.2}$$

Although experiments are carried out for three- [8–11] and two-dimensional [12] field configurations, detailed analytical calculations that have been performed for one-dimensional cooling [1, 2, 4] (an atom is driven by a pair of two counterpropagating laser beams) give a fairly accurate description of the major features of the cooling process. It has been shown that sub-Doppler-limit laser cooling is produced in the so-called lin⊥lin configuration, when the laser field consists of a pair of counterpropagating beams having orthogonal polarizations. For this configuration, the polarization gradient of the laser field plays a central role in the cooling process. This gradient results in different optical pumping rates and ac Stark shifts of the ground-state sublevels, both of which are spatially modulated. When an atom moves with a nonzero velocity along the laser-beam direction, it can be optically pumped, on average, from ac-Stark-shifted levels of lower energy to ac-Stark-shifted levels of higher energy, provided the sign of the atom-field detuning is chosen properly (so-called Sisyphus effect [1]). This optical pumping results in a damping of the atomic velocity. In general, the larger the spatial modulation of the difference in ac Stark shifts between the levels and the longer the optical pumping time, the stronger the frictional damping force. For weak fields, the optical pumping time τ_p can be made much larger than the excited-state lifetime Γ^{-1} resulting in a friction force that, for slow atoms, is much stronger than that in the case of Doppler cooling.

In the case of parallel linear polarizations for the fields, there is no field polarization gradient and the friction force is similar to that for Doppler cooling. One might think that as the rotation angle θ between the field's polarization vectors varies from 0 to $\pi/2$, the effectiveness of sub-Doppler-limit cooling would gradually increase, achieving its maximum for $\theta = \pi/2$. This conclusion is not necessarily correct. For small angles, $\theta \ll 1$, the intensity of the laser field varies considerably in space, and the optical pumping time strongly depends on the position of the atom. Although the ac Stark shifts differ only slightly for small θ, the fact that the optical-pumping time is increased significantly near regions of low field intensity can lead to a cooling force much stronger than that corresponding to $\theta = \pi/2$. Moreover, owing to the decrease in the difference of ac Stark shifts, the momentum diffusion coefficient that characterizes stochastic heating of atoms is much smaller for small angles than for $\theta = \pi/2$. The increase of the force and decrease of the diffusion may eventually lead to a lower equilibrium atomic kinetic energy for smaller angles, than for $\theta = \frac{\pi}{2}$, for a range of field intensities. It should be noted, however, that, if the field intensities are chosen to minimize the atomic kinetic energy, optimal cooling occurs for $\theta = \frac{\pi}{2}$.

It is the purpose of this paper to derive equations describing laser cooling of atoms having a $J = \frac{1}{2}$ ground state for arbitrary relative polarization angle θ. In deriving the results, one finds that standard computational techniques involving continued fractions or iterative solutions are not practical for a range of atomic velocities. An alternative analytical approach is used to solve for the atomic-state density-matrix elements.

In Sec. II a qualitative picture of sub-Doppler-limit cooling is given for an arbitrary relative polarization angle θ between the fields. The Fokker-Planck equation for the density matrix in the Wigner representation is derived in Sec. III. The results for the force, diffusion, and achievable temperatures are discussed in Sec. IV. Consequences and implications of the results obtained in this paper and related phenomena are discussed in Sec. V.

II. QUALITATIVE PICTURE

The laser field is represented by a pair of plane waves counterpropagating in the z direction. The direction of linear polarization of each field is shown in Fig. 1. The total electric-field amplitude is given by

$$\mathbf{E}(t;\mathbf{r}) = \mathbf{e}_1(Ee^{-i\omega t+ikz} + \text{c.c.}) + \mathbf{e}_2(Ee^{-i\omega t-ikz} + \text{c.c.}), \tag{2.1}$$

where the real amplitude E does not vary with time. In general, the unit polarization vectors $\mathbf{e}_1$ and $\mathbf{e}_2$ have different directions, so that

$$\mathbf{e}_1 = \cos\frac{\theta}{2}\mathbf{e}_x + \sin\frac{\theta}{2}\mathbf{e}_y, \tag{2.2}$$

$$\mathbf{e}_2 = \cos\frac{\theta}{2}\mathbf{e}_x - \sin\frac{\theta}{2}\mathbf{e}_y, \tag{2.3}$$

where the angle θ between the polarization vectors is restricted to $0 \leq \theta \leq \pi/2$.

The laser fields interact with an ensemble of atoms whose ground states g are characterized by total angular momentum $J_g = 1/2$. The ground states are linked by the nearly resonant laser fields to excited states e having total angular momentum $J_e = 1/2$ or $3/2$ [see Figs. 2(a) and 2(b), respectively]. Both cases are similar in many respects. To be specific, in the qualitative discussion we consider the case $J_e = 1/2$.

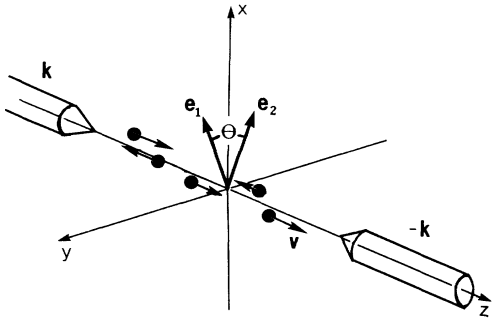

FIG. 1. One-dimensional field configuration. Two linearly polarized fields counterpropagate in the z direction with an angle θ between their polarization vectors.

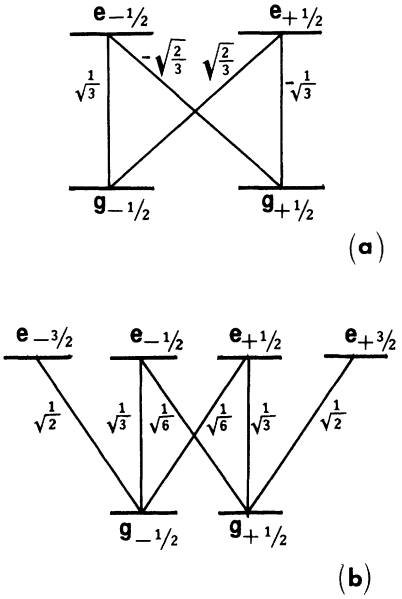

FIG. 2. Atomic level scheme and Clebsch-Gordan coefficients for (a) $J_g = \frac{1}{2} \rightarrow J_e = \frac{1}{2}$, and (b) $J_g = \frac{1}{2} \rightarrow J_e = \frac{3}{2}$ transitions.

It is convenient to represent the field (2.1) as a sum of two circularly polarized fields with polarizations $\mathbf{e}_\pm$ such that

$$\mathbf{e}_\pm = \frac{\mp\mathbf{e}_x - i\mathbf{e}_y}{\sqrt{2}}, \tag{2.4}$$

and amplitudes $E_\pm$ given by

$$E_\pm = \mp\sqrt{2}E\cos\left(kz \pm \frac{\theta}{2}\right)e^{-i\omega t}. \tag{2.5}$$

This system can be regarded as consisting of two two-level subsystems: $g - 1/2 \leftrightarrow e1/2$ and $g1/2 \leftrightarrow e - 1/2$, driven by the standing waves $E_\pm$ given by Eq. (2.5) and linked to each other by the transitions involving emission of spontaneous photons.

The force exerted by the fields on the atom is given by

$$F = \left\langle -\frac{dH_{\text{af}}}{dz} \right\rangle, \tag{2.6}$$

where H_{af} is the atom-field coupling given by Eq. (A5) of the Appendix, and where $\langle\ \rangle$ indicates a quantum mechanical average. In the weak-field limit defined by (1.1), one can adiabatically eliminate atomic density-matrix elements involving the excited state and obtain the force in the form

$$F = F_{\text{ext}} + F_{\text{int}}, \tag{2.7}$$

where

$$F_{\text{ext}} = -\frac{dU_0}{dz} = \frac{2\hbar\delta k f^2}{3(\delta^2 + \Gamma^2/4)}\cos\theta\sin(2kz) \tag{2.8}$$

and

$$F_{\rm int} = F_+\rho_+ + F_-\rho_- = -\frac{2\hbar\delta k f^2}{3(\delta^2+\Gamma^2/4)}\sin\theta\cos(2kz)\Pi. \quad (2.9)$$

The quantities appearing in Eqs. (2.8) and (2.9) are defined as follows: the Rabi frequency f has the form $f = \sqrt{2}E\mu/\hbar$; U_0 is an effective potential given by

$$U_0 = \frac{\hbar\delta f^2}{3(\delta^2+\Gamma^2/4)}\cos\theta\cos(2kz); \quad (2.10)$$

F_+ and F_- are equal to

$$F_+ = -F_- = -\frac{2\hbar k\delta f^2}{3(\delta^2+\Gamma^2/4)}\sin\theta\cos(2kz); \quad (2.11)$$

ρ_+ (ρ_-) is the population of the $m_J = 1/2$ ($m_J = -1/2$) ground-state magnetic sublevel; and Π is the population difference

$$\Pi = \rho_+ - \rho_-. \quad (2.12)$$

Consistent with the weak-field limit used to derive Eq.(2.7), the ground-state sublevel population is conserved, i.e.,

$$\rho_+ + \rho_- = 1. \quad (2.13)$$

Equation (2.7) is valid only in the limit of relatively small velocities,

$$|kv| \ll \max(\Gamma, |\delta|), \quad (2.14)$$

which is the only limit considered in this paper.

According to Eq. (2.7), the force consists of two components, an "external" part $F_{\rm ext}$ which is independent of the internal state of the atom, and an "internal" part $F_{\rm int}$, which depends on the population difference Π of the ground-state sublevels. The internal part can be written in terms of a force $F_\pm$ acting on each sublevel population. On averaging the force over an optical wavelength, the contribution of the external part vanishes, while that of the internal part depends on the Fourier component of Π, which varies as $\cos(2kz)$. Thus a determination of the spatially averaged force reduces to a determination of $\Pi(z)$.

The population difference Π is driven by the differential rate $(R_+ - R_-)$ at which atoms are optically pumped to the + and − ground-state sublevels, where, as shown explicitly in Sec. III, $R_\pm$ are given by

$$R_\pm = \frac{2\Gamma f_\pm^2}{9(\delta^2+\Gamma^2/4)} = \tau_p^{-1}\cos^2(kz \pm \tfrac{1}{2}\theta), \quad (2.15)$$

with

$$\tau_p = \frac{9(\delta^2+\Gamma^2/4)}{2\Gamma f^2}, \quad (2.16)$$

and $f_\pm = E_\pm\mu/\hbar$. The population difference relaxes back towards equilibrium at the rate $(R_+ + R_-)$. Under the weak-field condition (1.1), in steady state the population difference evolves as

$$v\frac{\partial\Pi}{\partial z} = (R_+ - R_-) - (R_+ + R_-)\Pi. \quad (2.17)$$

The driving term

$$R_+ - R_- = -\tau_p^{-1}\sin\theta\sin(2kz) \quad (2.18)$$

coincides with the difference of light shifts of ground-state sublevels. It is a periodic function of atomic position and is small in the vicinity of nodes ($kz \approx \pi/2 + \pi n$) and antinodes ($kz \approx \pi n$) of the field (the positions of "nodes" and "antinodes" to which we refer are those which would appear for parallel-polarized fields). The driving term vanishes for $\theta = 0$, implying that sub-Doppler-limit cooling does not occur for parallel polarizations of the fields. For $\theta \neq 0$ the driving term increases with increasing θ and reaches its maximum value for laser beams having orthogonal polarization ($\theta = \frac{\pi}{2}$).

The local optical relaxation rate $R_{\rm loc}$ for the population difference of the sublevels is equal to

$$R_{\rm loc} = R_+ + R_- = \tau_p^{-1}[1 + \cos\theta\cos(2kz)]. \quad (2.19)$$

In the case of orthogonal polarization $\theta = \frac{\pi}{2}$, this rate does not depend on position z. However, for small angles $\theta \ll 1$, $R_{\rm loc}$ is strongly position dependent, and is very small near the nodes of the field (that is, relaxation of the ground-state sublevel population difference is slow in these regions). Although the driving term (2.18) is also small in the vicinity of the nodes, the competition of these two small quantities leads to a considerable gradient of the population difference. It is the rapid variation of $R_{\rm loc}$ near the field nodes that may lead to qualitatively new features in laser cooling.

To understand the qualitative features of the spatially averaged force, we first consider atoms having $v = 0$. Although these atoms do not experience the averaged force, it follows from Eqs. (2.7) and (2.17) that, for sufficiently slow atoms, the spatially averaged force can be obtained in terms of the gradient of the population difference of $v = 0$ atoms. From Eq. (2.17) one finds this population difference to be given by

$$\Pi(x, v=0) = -\frac{\sin\theta\sin 2kz}{1+\cos\theta\cos 2kz}. \quad (2.20)$$

For $\theta = \pi/2$, $\Pi(z, v=0) = -\sin(2kz)$. Defining a characteristic scale $z_{\rm sc}$ over which Π varies as

$$z_{\rm sc} \approx \Pi/(d\Pi/dz), \quad (2.21)$$

one sees that $z_{\rm sc} \sim k^{-1}$ when $\theta = \pi/2$ (see curve 1 in Fig. 3). However, for small angles $\theta \ll 1$, a new length scale is introduced into the problem. Far from the field nodes ($|kz - \frac{\pi}{2}(1+2n)| \gg \theta$, $n = 0, \pm 1, \ldots$) the population difference is small:

$$\Pi(z, v=0) = -\theta\tan kz, \quad (2.22)$$

while, in the vicinity of the nodes, $\Pi(z, v=0)$ takes the form

$$\Pi(z, v=0) = \frac{\theta\epsilon}{(\theta/2)^2+\epsilon^2}, \quad (2.23)$$

where $\epsilon = kz - (1+2n)\pi/2$. One can see from Eq. (2.23) and curve 2 in Fig. 3 that, in contrast to the $\theta = \pi/2$ case, for small θ, near the nodes the population difference is of order unity and varies very rapidly on a scale $z_{\rm sc} \sim \frac{\theta}{2k}$.

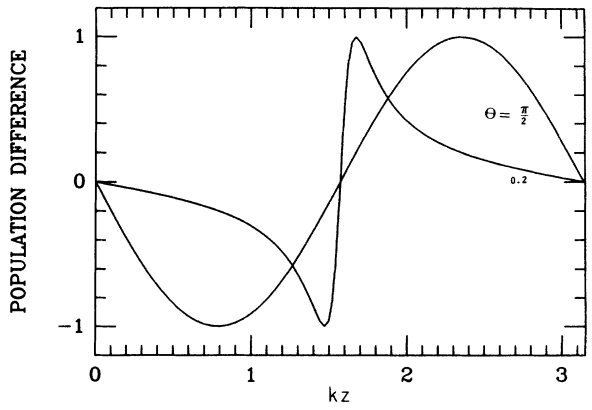

FIG. 3. The population difference $\Pi(z, v = 0)$ of the ground-state sublevels as a function of kz for $\theta = \frac{\pi}{2}$ and $\theta = 0.2$. The value $kz = \frac{\pi}{2}$ corresponds to a field node.

Next we consider an atom moving in the z direction with a very small velocity v, such that Π does not vary considerably during an optical pumping period, that is,

$$v \ll R_{\rm loc} z_{\rm sc}. \tag{2.24}$$

In this limit the velocity-dependent part Π_v of the population difference grating which gives rise to a nonvanishing averaged force can be obtained from Eq. (2.17) by a standard one-step iteration, and is given by

$$\Pi_v = -vR_{\rm loc}^{-1}\frac{d\Pi(z, v = 0)}{dz} = \frac{2kv\tau_p(\cos\theta + \cos 2kz)}{(1 + \cos\theta\cos 2kz)^3}. \tag{2.25}$$

Atoms having velocities v satisfying inequality (2.24) give rise to a spatially averaged force that varies linearly with v (so-called "capture range" of the force [13]). One can see from Eq. (2.25) that a decrease in the optical relaxation rate and an increase of the population difference gradient lead to larger Π_v (see Fig. 4) and might thus lead to stronger averaged force. Owing to the dependence of $R_{\rm loc}$ on θ, both the capture range defined by (2.24) and the magnitude of the force depend strongly on θ.

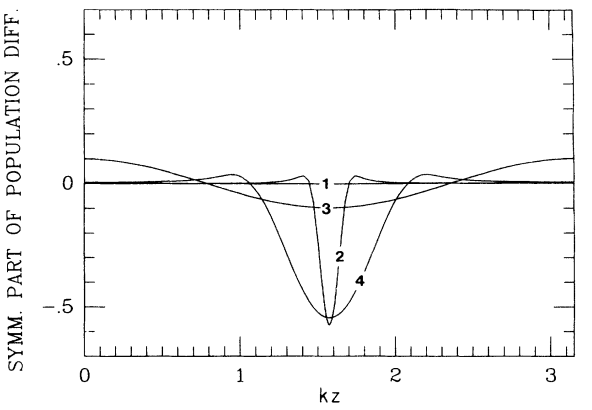

FIG. 4. Velocity-dependent part of the population difference $\Pi(z, v)$ that contributes to the spatially averaged force, as a function of kz for several values of θ and $\alpha = kv\tau_p$. (1) $\theta = \frac{\pi}{2}, \alpha = 1.0 \times 10^{-3}$; (2) $\theta = 0.2, \alpha = 1.0 \times 10^{-3}$; (3) $\theta = \frac{\pi}{2}, \alpha = 5 \times 10^{-2}$; (4) $\theta = 0.2, \alpha = 5 \times 10^{-2}$.

For the fields with orthogonal polarization ($\theta = \pi/2$), one has $R_{\rm loc}^{-1} = \tau_p$, and Eq. (2.24) takes the form

$$\alpha \equiv kv\tau_p \ll 1. \tag{2.26}$$

In this limit one obtains the well-known result [1] for the friction force

$$\bar{F} = -\frac{2\hbar k f^2 \delta\alpha}{3(\delta^2 + \Gamma^2/4)}. \tag{2.27}$$

For small θ, both the local optical relaxation rate and the spatial scale over which the population difference varies decrease near the field nodes, so that $R_{\rm loc} \sim \tau_p^{-1}\theta^2/2$ and $z_{\rm sc} \sim \theta/2$. It follows from Eqs.(2.19) and (2.24) that the capture range is given by

$$\alpha \ll \theta^3 \tag{2.28}$$

and is much smaller than that for $\theta = \frac{\pi}{2}$. In this capture range, however, the strong gradient of Π and long optical-pumping time in the vicinity of the field nodes give rise to a spatially averaged force

$$\bar{F} = -\frac{2\hbar k f^2 \delta\alpha}{3\theta(\delta^2 + \Gamma^2/4)}, \tag{2.29}$$

which is larger than that for $\theta = \frac{\pi}{2}$. For small θ and v the entire contribution to the force originates when an atom moves near the field nodes.

The iterative approach used to arrive at Eq. (2.25) is only applicable when condition (2.24) is satisfied. In the case of orthogonal field polarization, condition (2.24) is satisfied provided that $\alpha = kv\tau_p \ll 1$; however, for $\theta \ll 1$ this condition is satisfied only for $\alpha = kv\tau_p \ll \theta^3$. Thus for $\theta \ll 1$ there exists a range of velocities

$$1 \gg \alpha \gg \theta^3, \tag{2.30}$$

for which the iterative approach fails. These velocities are high enough to prevent the population difference of the ground-state sublevels to undergo considerable relaxation during the passage through the field node, but low enough for this process to occur at a spatial scale smaller than the optical wavelength. For this velocity range, a theoretical approach based on a Fourier series expansion for Π is not of much practical use either, since the number of terms involved is prohibitively large. New analytical techniques are needed, which are described in the subsequent sections.

Nevertheless, it is possible to obtain a qualitative picture of the velocity dependence for the force in the range (2.30) by introducing the concept of an effective optical relaxation rate $R_{\rm eff}$ defined by

$$\int_{t - R_{\rm eff}^{-1}}^{t} R_{\rm loc}(t')dt' = 1, \tag{2.31}$$

where $t = (z - z_0)/v$, and $R_{\rm loc}$ is given by Eq. (2.19). Equation (2.31) simply states that the probability of optical pumping in the time interval $(t - R_{\rm eff}^{-1}, t)$ is equal

to unity. For the range of atomic velocities satisfying inequalities (2.30), in the vicinity of the nodes, integration of Eq. (2.31) leads to the effective optical relaxation rate

$$R_{\rm eff} \sim \tau_p^{-1}[\epsilon^2 + (\tfrac{2}{3}\alpha)^{2/3}] \ll \tau_p^{-1}, \tag{2.32}$$

which does not depend on θ and increases with increasing velocity. The spatial scale of the population difference is now given by $z_{\rm sc} = vR_{\rm eff}^{-1} \sim \alpha^{1/3}/k$ (see curve 4 in Fig. 4). The largest contribution to the spatially averaged force is produced in a single optical-pumping cycle when an atom passes the field node. In the range of velocities (2.30) the averaged force is given by

$$\bar{F} \approx -\frac{\hbar k f^2 \delta \sin^2\theta}{3\sqrt{3}(\delta^2 + \Gamma^2/4)} \tag{2.33}$$

and is independent of v.

A graph of $\bar{F}$ vs θ for small $\alpha \ll 1$ is shown in Fig. 5. The force first increases with increasing θ, and reaches its maximum value for a small angle $\theta \sim \alpha^{1/3}$. Then it decreases, approaching the value $\bar{F}(\theta = \pi/2, v)$ as θ tends to $\pi/2$.

We now turn our attention to the momentum diffusion coefficient D, which consists of two parts:

$$D = D_{\rm sp} + D_{\rm ind}, \tag{2.34}$$

The first contribution $D_{\rm sp}$ is related to the fluctuations concerned with emission of spontaneous photons. This contribution is quite similar to the momentum diffusion coefficient in a two-level system. For $|kv| \ll \Gamma$, it depends only slightly on angle and velocity, since the specific features of sub-Doppler-limit cooling and multilevel dynamics do not play a significant role in the diffusion processes brought about by these fluctuations. The averaged contribution $\bar{D}_{\rm sp}$ can be roughly estimated by

$$\bar{D}_{\rm sp} \sim \frac{\hbar^2 k^2}{\tau_p}. \tag{2.35}$$

The second contribution $D_{\rm ind}$ is produced by the fluctuations of the stimulated force exerted on the atom, and is given by

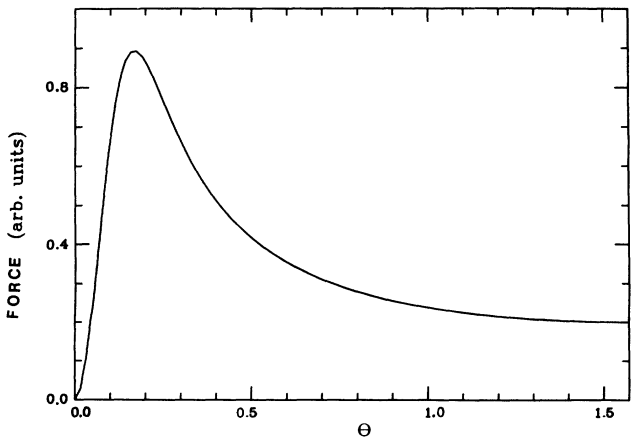

FIG. 5. The spatially averaged laser cooling force as a function of angle θ for small $\alpha = kv\tau_p = 1.0 \times 10^{-3}$.

$$D_{\rm ind} = \int_{-\infty}^{0} [\langle F(t)F(t-\tau)\rangle - \langle F(t)\rangle\langle F(t-\tau)\rangle]d\tau. \tag{2.36}$$

This contribution is directly related to the multilevel dynamics, since it is brought about by fluctuations in the time periods an atom stays in sublevels $m_J = \pm 1/2$ of the ground state. For relatively small velocities satisfying the condition $\alpha \ll 1$, the correlation time of the forces in Eq. (2.36) is given by $R_{\rm eff}^{-1}$, and $D_{\rm ind}$ is approximately equal to

$$D_{\rm ind} \approx \frac{F_+^2}{R_{\rm eff}}, \tag{2.37}$$

where F_+ is given by Eq. (2.11).

For $\theta \ll 1$, the force F_+ is θ times smaller than that for $\theta = \frac{\pi}{2}$. On the other hand, in the vicinity of the field nodes, $R_{\rm eff} \ll \tau_p^{-1}$. The overall effect is a decrease of the averaged diffusion coefficient with decreasing θ, given by

$$\bar{D}_{\rm ind}(\theta, v) \sim \frac{\theta\delta^2}{\Gamma^2}\bar{D}_{\rm sp} \tag{2.38}$$

for very slow atoms satisfying Eq. (2.28), and

$$\bar{D}_{\rm ind}(\theta, v) \sim \frac{\theta^2\delta^2}{\alpha^{1/3}\Gamma^2}\bar{D}_{\rm sp} \tag{2.39}$$

for intermediate velocities (2.30). Thus, for small θ, the induced momentum diffusion coefficient $\bar{D}_{\rm ind}(\theta \ll 1, v)$ is much smaller than $\bar{D}_{\rm ind}(\theta = \pi/2, v)$. It also exhibits significant dependence on velocity v in the range $\theta^3 \ll \alpha \ll 1$. The consequences of the θ dependences of $\bar{F}$ and $\bar{D}$ are discussed below.

III. EQUATIONS FOR THE GROUND-STATE SUBLEVEL POPULATIONS

In this section, using the Wigner representation [14], we derive the equations for the populations of the ground-state sublevels. We consider atoms having ground- and excited-state angular momenta $J_g = \frac{1}{2}$ and $J_e = \frac{1}{2}$ or $\frac{3}{2}$. Using the general equations (see, for instance, [14,4]) for the density matrix $\rho(z,p)$, where $p = Mv$ is the atomic momentum, and z is the center-of-mass position, and taking into account the weak-field condition (1.1), one can adiabatically eliminate excited-state matrix elements and obtain a closed set of equations for the density-matrix elements of the ground state [1, 4]. The derivation of the equations is given in the Appendix and is quite similar for the two values of J_e. Assuming that the atomic momentum is much larger than that of the photon, that is

$$p \gg \hbar k, \tag{3.1}$$

one finds the following equations for the ground-state sublevel populations:

$$\frac{d}{dt}\rho_{\pm} = \frac{2\Gamma f^2}{9(\delta^2+\Gamma^2/4)}\left[-\cos^2\left(\mp\frac{\theta}{2}+kz\right)\rho_{\pm}+\cos^2\left(\pm\frac{\theta}{2}+kz\right)\rho_{\mp}-\frac{3\hbar k\delta}{\Gamma}\sin(\mp\theta+2kz)\frac{\partial\rho_{\pm}}{\partial p}\right.$$
$$\left.+\frac{\hbar^2k^2}{20}\left([14-11\cos(\mp\theta+2kz)]\frac{\partial^2\rho_{\pm}}{\partial p^2}+[6+\cos(\pm\theta+2kz)]\frac{\partial^2\rho_{\mp}}{\partial p^2}\right)\right] \tag{3.2}$$

for $J_e=\frac{1}{2}$, and

$$\frac{d}{dt}\rho_{\pm} = \frac{\Gamma f^2}{9(\delta^2+\Gamma^2/4)}\left[-\cos^2\left(\mp\frac{\theta}{2}+kz\right)\rho_{\pm}+\cos^2\left(\pm\frac{\theta}{2}+kz\right)\rho_{\mp}-\frac{3\hbar k\delta}{2\Gamma}[\sin(\mp\theta+2kz)+3\sin(\pm\theta+2kz)]\frac{\partial\rho_{\pm}}{\partial p}\right.$$
$$\left.+\frac{\hbar^2k^2}{40}\left([70-13\cos(\mp\theta+2kz)-27\cos(\pm\theta+2kz)]\frac{\partial^2\rho_{\pm}}{\partial p^2}+2[6+\cos(\pm\theta+2kz)]\frac{\partial^2\rho_{\mp}}{\partial p^2}\right)\right] \tag{3.3}$$

for $J_e=\frac{3}{2}$, where $d/dt=\partial/\partial t+v\partial/\partial z$. Equations (3.2) and (3.3) provide a complete description of the time evolution of the atomic distribution of ground-state sublevels as a function of atomic center-of-mass position and momentum, in the limit of weak field (1.1) and small photon momentum (3.1). The first two terms on the right-hand side of the equations describe the spatially dependent population exchange between the sublevels owing to the optical pumping. The term with $\partial/\partial p$ can be interpreted as a gradient of an effective potential determined by the spatially dependent ac Stark shifts of the levels,

$$S_{\pm} = -\frac{\hbar\delta f^2}{3(\delta^2+\Gamma^2/4)}\cos(\mp\theta+2kz) \tag{3.4}$$

for $J_e=\frac{1}{2}$, and

$$S_{\pm} = -\frac{\hbar\delta f^2}{12(\delta^2+\Gamma^2/4)}[\cos(\mp\theta+2kz)+3\cos(\pm\theta+2kz)] \tag{3.5}$$

for $J_e=\frac{3}{2}$. Finally, the terms containing the second derivatives with respect to p correspond to the momentum diffusion process caused by emission of spontaneous photons.

To find the atomic momentum and position distributions it is useful to introduce the probability density

$$\psi(z,p)=\rho_{+}+\rho_{-} \tag{3.6}$$

for an atom to have momentum p and position z, and the population difference density

$$\Pi(z,p)=\rho_{+}-\rho_{-}. \tag{3.7}$$

Then, using Eq. (3.2) with $J_e=\frac{1}{2}$, one arrives at

$$\frac{d}{dt}\psi = \frac{1}{\tau_p}\left[-\frac{3\hbar k\delta}{\Gamma}\left(\cos\theta\sin 2kz\frac{\partial\psi}{\partial p}-\sin\theta\cos 2kz\frac{\partial\Pi}{\partial p}\right)\right.$$
$$\left.+\frac{\hbar^2k^2}{2}\left((2-\cos\theta\cos 2kz)\frac{\partial^2\psi}{\partial p^2}-\sin\theta\sin 2kz\frac{\partial^2\Pi}{\partial p^2}\right)\right] \tag{3.8}$$

and

$$\frac{d}{dt}\Pi = \frac{1}{\tau_p}\left[-\psi\sin\theta\sin 2kz-(1+\cos\theta\cos 2kz)\Pi\right.$$
$$+\frac{3\hbar k\delta}{\Gamma}\left(\sin\theta\cos 2kz\frac{\partial\psi}{\partial p}-\cos\theta\sin 2kz\frac{\partial\Pi}{\partial p}\right)$$
$$\left.+\frac{\hbar^2k^2}{5}\left((2-3\cos\theta\cos 2kz)\frac{\partial^2\Pi}{\partial p^2}-3\sin\theta\sin 2kz\frac{\partial^2\psi}{\partial p^2}\right)\right], \tag{3.9}$$

where the "optical pumping" time τ_p is defined by Eq. (2.16). Similar equations can be obtained for $J_e=\frac{3}{2}$ using Eq. (3.3).

In general, Eqs. (3.2) and (3.3) or (3.8) and (3.9) cannot be further simplified. However, if the atomic kinetic energy $E_k=p^2/2M$ is much larger than the effective potentials $S_{\pm}$, that is if

$$\frac{p^2}{2M}\gg\frac{2\hbar\delta f^2}{3(\delta^2+\Gamma^2/4)}, \tag{3.10}$$

the atoms move almost freely and localization effects are weak. This implies that the time scale τ_E that characterizes the time variation of $\psi(z,p)$ satisfies the condition

$$\tau_E kv\gg 1. \tag{3.11}$$

As a consequence, the probability $\psi(z,p)=\rho_{+}+\rho_{-}$ depends only slightly on z. Below we neglected this dependence [15]. The problem is then reduced to a determination of the atomic momentum distribution $\psi(p)\equiv\psi(z,p)$. To obtain $\psi(p)$ as a solution of Eq. (3.8), one must know the population difference density $\Pi(z,p)$. The steady-state distribution for the population difference Π_{SS} is established on a time scale $R_{\rm eff}^{-1}$ given by Eq. (2.31). Although, as has been discussed in Sec. II, $R_{\rm eff}$ may vary significantly with atomic position and velocity,

it can be shown (see below) that $R_{\text{eff}}^{-1} \ll \tau_E$. In determining $\psi(p)$ from Eq. (3.8), one is then justified in replacing Π in that equation by its steady-state value Π_{SS}. Taking into account the condition $E_k \gg S_\pm$ and neglecting terms containing $\partial\Pi/\partial p$, and $\partial^2\psi/\partial p^2$and $\partial^2\Pi/\partial p^2$ in Eq. (3.9) [owing to conditions (3.1) and (3.10), respectively], one finds the steady-state solution of Eq. (3.9) in the form

$$\Pi_{SS}(z,p) = \frac{1}{2\alpha}\int_0^\infty dz' \left(-\sin\theta\sin(2kz-z')\psi(z,p) + \frac{3\hbar k\delta}{\Gamma}\sin\theta\cos(2kz-z')\frac{\partial\psi(z,p)}{\partial p}\right) \times \exp\left(-(2\alpha)^{-1}\int_0^{z'}[1+\cos\theta\cos(2kz-z'')]dz''\right), \tag{3.12}$$

where

$$\alpha = kv\tau_p. \tag{3.13}$$

Substituting $\Pi_{SS}(z,p)$ in the form (3.12) into Eq. (3.8) and neglecting derivatives of order higher than 2, one arrives at a Fokker-Planck equation of the form

$$\frac{d}{dt}\psi = \frac{\partial}{\partial p}[-F\,\psi + D_{\text{ind}}\frac{\partial\psi}{\partial p} + \frac{\partial}{\partial p}(D_{\text{sp}}\psi)], \tag{3.14}$$

where the force F is given by

$$F = \frac{2\hbar k\delta f^2}{3(\delta^2+\Gamma^2/4)}\left[\cos\theta\sin 2kz + (2\alpha)^{-1}\sin^2\theta\cos 2kz \times \int_0^\infty dz'\sin(2kz-z')\exp\left(-(2\alpha)^{-1}\int_0^{z'}[1+\cos\theta\cos(2kz-z'')]dz''\right)\right], \tag{3.15}$$

the sub-Doppler-limit "stimulated" contribution D_{ind} to the momentum diffusion produced by the fluctuations of the instantaneous dipole forces by

$$D_{\text{ind}} = \frac{1}{2\alpha\tau_p}\left(\frac{3\hbar k\delta\sin\theta}{\Gamma}\right)^2\cos 2kz\int_0^\infty dz'\cos(2kz-z')\exp\left(-(2\alpha)^{-1}\int_0^{z'}[1+\cos\theta\cos(2kz-z'')]dz''\right), \tag{3.16}$$

and the "spontaneous" contribution D_{sp} to the momentum diffusion associated with emission of spontaneous photons by

$$D_{\text{sp}} = \frac{\hbar^2k^2}{2\tau_p}\left[2-\cos\theta\cos 2kz + \frac{\sin^2\theta\sin 2kz}{2\alpha}\int_0^\infty dz'\sin(2kz-z')\exp\left(-(2\alpha)^{-1}\int_0^{z'}[1+\cos\theta\cos(2kz-z'')]dz''\right)\right]. \tag{3.17}$$

Under assumption (3.10) considerable variation in atomic kinetic energy occurs on a time scale larger than $(kv)^{-1}$. In other words, condition (3.11) is satisfied. In this limit, the force and diffusion averaged over a wavelength determine the time evolution of the distribution ψ. Averaging Eqs. (3.15)–(3.17) over a wavelength, and substituting the results into Eq. (3.14), one can arrive at

$$\frac{\partial\psi}{\partial t} = \frac{\partial}{\partial p}[-\bar{F}\,\psi + \bar{D}_{\text{ind}}\frac{\partial\psi}{\partial p} + \frac{\partial}{\partial p}(\bar{D}_{\text{sp}}\psi)], \tag{3.18}$$

where the spatially averaged force $\bar{F}$ is given by

$$\bar{F} = -\frac{\hbar kf^2\delta\sin^2\theta}{3(\delta^2+\Gamma^2/4)}\int_0^\infty \sin(2\alpha\tau)e^{-\tau}I_0\left(\frac{\cos\theta}{\alpha}\sin(\alpha\tau)\right)d\tau, \tag{3.19}$$

and the averaged diffusion coefficients are

$$\bar{D}_{\text{sp}} = \frac{2\hbar^2k^2f^2\Gamma}{9(\delta^2+\Gamma^2/4)}\left\{1+\frac{1}{4}\sin^2\theta\int_0^\infty e^{-\tau}\left[\cos(2\alpha\tau)I_0\left(\frac{\cos\theta}{\alpha}\sin(\alpha\tau)\right) - I_2\left(\frac{\cos\theta}{\alpha}\sin(\alpha\tau)\right)\right]d\tau\right\}, \tag{3.20}$$

$$\bar{D}_{\text{ind}} = \frac{\hbar^2k^2\delta^2f^2\sin^2\theta}{\Gamma(\delta^2+\Gamma^2/4)}\int_0^\infty e^{-\tau}\left[\cos(2\alpha\tau)I_0\left(\frac{\cos\theta}{\alpha}\sin(\alpha\tau)\right) + I_2\left(\frac{\cos\theta}{\alpha}\sin(\alpha\tau)\right)\right]d\tau, \tag{3.21}$$

where I_0 and I_2 are modified Bessel functions [16].

For $J_e = \frac{3}{2}$, one can also obtain equations similar to Eqs. (3.14) and (3.18). For example, the force F is given by

$$F = \frac{\hbar k \delta f^2}{3(\delta^2 + \Gamma^2/4)} \left[2\cos\theta \sin 2kz - (4\alpha)^{-1} \sin^2\theta \cos 2kz \right.$$
$$\left. \times \int_0^\infty dz' \sin(2kz - z') \exp\left(-(4\alpha)^{-1} \int_0^{z'} [1 + \cos\theta \cos(2kz - z'')] dz'' \right) \right] , \tag{3.22}$$

and the averaged force $\bar{F}$ by

$$\bar{F} = \frac{\hbar k f^2 \delta \sin^2\theta}{6(\delta^2 + \Gamma^2/4)} \int_0^\infty \sin(4\alpha\tau) e^{-\tau} I_0 \left(\frac{\cos\theta}{2\alpha} \sin(2\alpha\tau) \right) d\tau . \tag{3.23}$$

For the sub-Doppler-limit stimulated part of the momentum diffusion coefficients one finds

$$D_{\text{ind}} = \frac{1}{2\alpha\tau_p} \left(\frac{3\hbar k \delta \sin\theta}{2\Gamma} \right)^2 \cos 2kz \int_0^\infty \cos(2kz - z') \exp\left(-(4\alpha)^{-1} \int_0^{z'} [1 + \cos\theta \cos(2kz - z'')] dz'' \right) dz', \tag{3.24}$$

and

$$\bar{D}_{\text{ind}} = \frac{\hbar^2 k^2 \delta^2 f^2 \sin^2\theta}{2\Gamma(\delta^2 + \Gamma^2/4)} \int_0^\infty e^{-\tau} \left[\cos(4\alpha\tau) I_0 \left(\frac{\cos\theta}{2\alpha} \sin(2\alpha\tau) \right) + I_2 \left(\frac{\cos\theta}{2\alpha} \sin(2\alpha\tau) \right) \right] d\tau, \tag{3.25}$$

while the spontaneous contribution D_{sp} to the momentum diffusion is given by

$$D_{\text{sp}} = \frac{\hbar^2 k^2}{40\tau_p} \left[41 - 19\cos\theta \cos 2kz - \frac{2\sin^2\theta \sin 2kz}{\alpha} \right.$$
$$\left. \times \int_0^\infty dz' \sin(2kz - z') \exp\left(-(4\alpha)^{-1} \int_0^{z'} [1 + \cos\theta \cos(2kz - z'')] dz'' \right) \right] \tag{3.26}$$

and

$$\langle D_{\text{sp}} \rangle = \frac{\hbar^2 k^2 f^2 \Gamma}{20(\delta^2 + \Gamma^2/4)} \left\{ 41 - 4\sin^2\theta \int_0^\infty e^{-\tau} \left[\cos(4\alpha\tau) I_0 \left(\frac{\cos\theta}{2\alpha} \sin(2\alpha\tau) \right) - I_2 \left(\frac{\cos\theta}{2\alpha} \sin(2\alpha\tau) \right) \right] d\tau \right\} . \tag{3.27}$$

IV. DISCUSSION

In this section, if not stated otherwise, we consider $J_e = \frac{1}{2}$.

A. Force and diffusion

For $\theta = \frac{\pi}{2}$ one can use Eqs. (3.19)–(3.21) to obtain expressions for the force and momentum diffusion coefficients in a closed form for arbitrary values of the dimensionless velocity $\alpha = kv\tau_p$. For the averaged force one recovers the well-known result [1]

$$\bar{F}\left(\theta = \frac{\pi}{2}\right) = -\frac{2\hbar k f^2 \delta \alpha}{3(\delta^2 + \Gamma^2/4)(1 + 4\alpha^2)} . \tag{4.1}$$

The diffusion coefficients are given by

$$\bar{D}_{\text{ind}}\left(\theta = \frac{\pi}{2}\right) = \frac{\hbar^2 k^2 \delta^2 f^2}{\alpha(\delta^2 + \Gamma^2/4)(1 + 4\alpha^2)} \tag{4.2}$$

and

$$\bar{D}_{\text{sp}}\left(\theta = \frac{\pi}{2}\right) = \frac{2\hbar^2 k^2 f^2 \Gamma}{9(\delta^2 + \Gamma^2/4)} \left(1 + \frac{1}{4(1 + 4\alpha^2)} \right) , \tag{4.3}$$

and their qualitative behavior coincides with that of diffusion coefficients obtained in Ref. [4].

For an arbitrary angle θ, it is possible to obtain analytical expressions for the averaged force and diffusion coefficients in the limiting cases of small and large velocities. Numerical solutions for the force and the diffusion coefficients as a function of α are presented in Figs. 6 and 7, respectively.

1. *Low velocities* $\alpha \ll 1$

In this limit, for very low velocities

$$\alpha \ll \frac{\theta^3}{6} , \tag{4.4}$$

one can take the integrals in Eqs.(3.19)–(3.21) to obtain

$$\bar{F} = -\frac{2\hbar k f^2 \delta \alpha}{3\sin\theta(\delta^2 + \Gamma^2/4)} \tag{4.5}$$

and

$$\bar{D} = \bar{D}_{st} + \bar{D}_{sp} = \frac{\hbar^2 k^2 f^2 \Gamma}{9(\delta^2 + \Gamma^2/4)} \times \left(2 + \frac{\sin^2\theta}{1+\sin\theta} + \frac{18\delta^2}{\Gamma^2}\frac{\sin\theta}{1+\sin\theta}\right) . \tag{4.6}$$

The force increases and the diffusion coefficient decreases gradually with decreasing θ.

In particular, for small angles $\theta \ll 1$ and very small velocities satisfying (4.4), one finds

$$\bar{F} = -\frac{2\hbar k f^2 \delta \alpha}{3\theta(\delta^2 + \Gamma^2/4)} = -\frac{3\hbar k^2 \delta v}{\theta\Gamma} \tag{4.7}$$

and

$$\bar{D} = \frac{2\hbar^2 k^2 f^2 \Gamma}{9(\delta^2 + \Gamma^2/4)}\left(1 + \frac{9\delta^2\theta}{\Gamma^2}\right) . \tag{4.8}$$

The force increases as θ^{-1} and the diffusion coefficient decreases linearly with decreasing θ.

To determine the source of such a strong dependence of the force and diffusion on θ, one can examine the expressions (3.15)–(3.17) for the nonaveraged force and diffusion. If condition (4.4) is satisfied, one has

$$F \approx \frac{2\hbar k \delta f^2}{3(\delta^2 + \Gamma^2/4)}\left[\cos\theta \sin 2kz + \sin^2\theta\left(\frac{\sin 4kz}{2(1+\cos\theta\cos 2kz)} - \frac{2\alpha\cos 2kz(\cos 2kz + \cos\theta)}{(1+\cos\theta\cos 2kz)^3}\right)\right] . \tag{4.9}$$

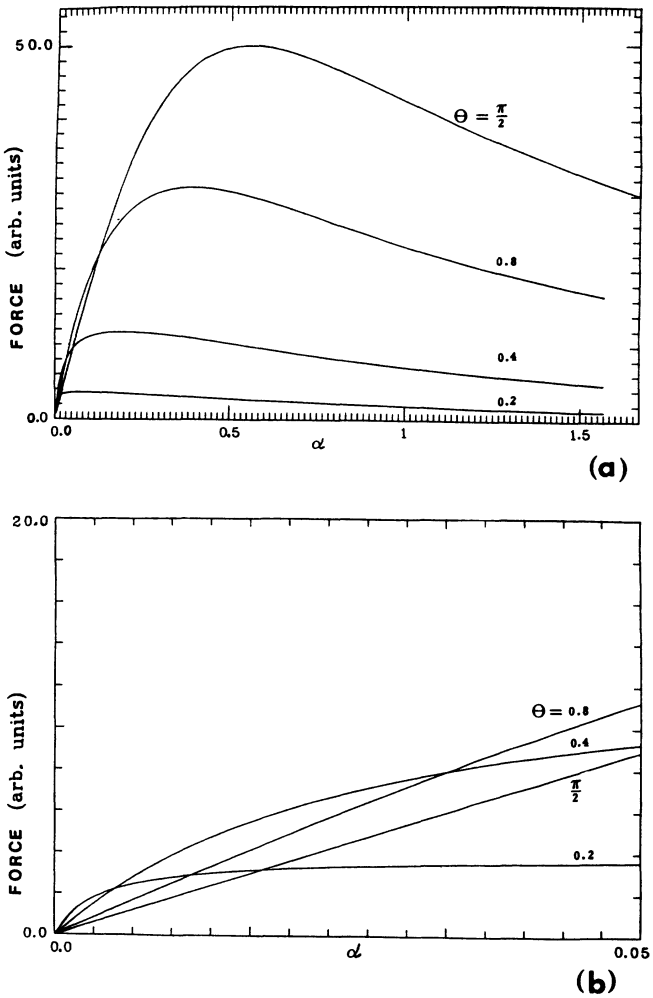

FIG. 6. Spatially averaged laser cooling force as a function of $\alpha = kv\tau_p$. The different curves correspond to different angles θ between the fields' polarization directions. The atomic transition occurs between two levels, each having total angular momentum $J = \frac{1}{2}$, and $\delta = 5\Gamma$. The force for very low velocities is shown in more detail in (b).

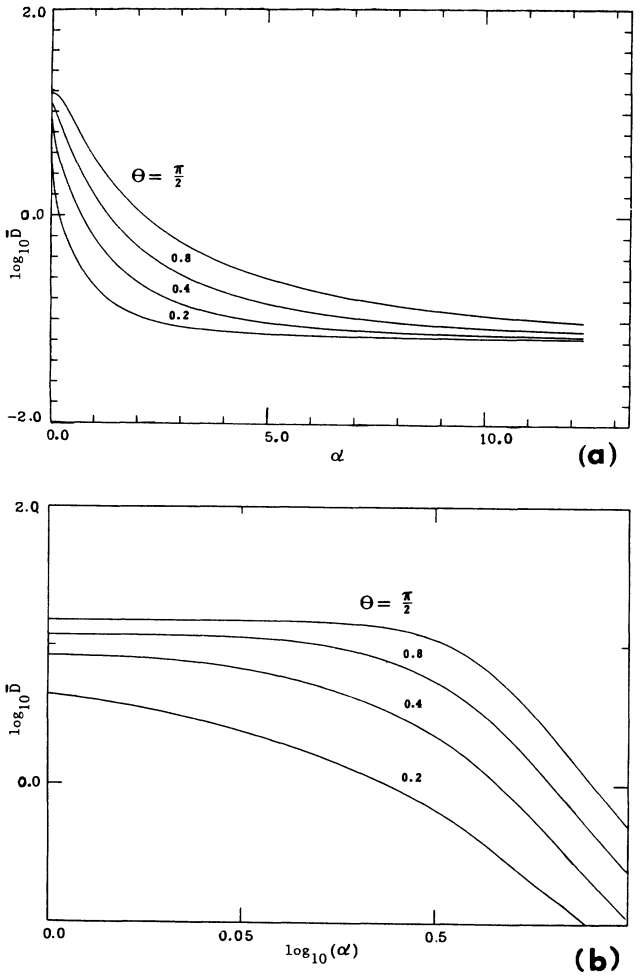

FIG. 7. The spatially averaged momentum diffusion coefficient as a function of $\alpha = kv\tau_p$. The different curves correspond to different angles θ between the fields' polarization directions. The atomic transition occurs between two levels, each having total angular momentum $J = \frac{1}{2}$, and $\delta = 5\Gamma$. The momentum diffusion coefficient for very low velocities is shown in more detail in (b).

For $\theta \ll 1$, far from the nodes of the standing wave [$|kz - \frac{\pi}{2}(1+2n)| \sim 1$] the velocity-dependent part of the force (4.9) is of order $\theta^2\hbar k^2\delta v/\Gamma$ and is much smaller than that of the force obtained for $\theta = \pi/2$. However, in the vicinity of the nodes, where

$$\epsilon = kz - \frac{\pi}{2}(1+2n) \ll 1, \tag{4.10}$$

the force takes the form

$$F \approx \frac{2\hbar k\delta f^2}{3(\delta^2+\Gamma^2/4)}\left(\frac{2\epsilon(\theta^2/4-\epsilon^2)}{(\epsilon^2+\theta^2/4)} - \frac{\theta^2\alpha(\theta^2/4-\epsilon^2)}{2(\epsilon^2+\theta^2/4)^3}\right). \tag{4.11}$$

The first term in Eq. (4.11) is velocity independent and corresponds to the gradient of the effective potential $U_{\rm eff}$ given by

$$U_{\rm eff} = \frac{2\hbar\delta f^2}{3(\delta^2+\Gamma^2/4)}\left(\epsilon^2 - \frac{\theta^2}{2}\ln(\epsilon^2+\theta^2/4)\right). \tag{4.12}$$

The second, velocity-dependent, term can be seen in Fig. 4 (curve 2). In the very vicinity of the node $\epsilon \ll \theta$, it represents a very strong frictional force

$$F_v \approx -\frac{24\hbar k^2\delta v}{\theta^2\Gamma}, \tag{4.13}$$

while for $|\epsilon| > \theta/2$ it changes sign and leads to heating. However, after averaging over the position around the node the combined effect is still that of cooling given by Eq. (4.7). Thus one can see that for small θ a strong frictional force is produced in vicinities close to the standing wave nodes.

The nonaveraged sub-Doppler-limit stimulated contribution $D_{\rm ind}$ to the momentum diffusion is proportional to θ^2 far from the nodes and is much smaller than that in the case $\theta = \pi/2$. However, near the field nodes [i.e., when condition (4.10) is satisfied], $D_{\rm ind}$ is given by

$$D_{\rm ind} = \frac{1}{2\tau_p}\left(\frac{3\hbar k\delta\theta}{\Gamma}\right)^2\frac{1}{\epsilon^2+\theta^2/4}. \tag{4.14}$$

For $\epsilon < \theta$, $D_{\rm ind}(\theta \ll 1)$ is of the order of $D_{\rm ind}(\theta = \pi/2)$ and provides the major contribution to the averaged diffusion coefficient (3.16).

For the intermediate range of velocities

$$1 \gg \alpha > \frac{\theta^3}{6} \tag{4.15}$$

the averaged force takes the form

$$\bar{F} = -\frac{2\hbar k f^2\delta\theta^2}{3\sqrt{3}(\delta^2+\Gamma^2/4)}. \tag{4.16}$$

Thus, for $\theta^3/6 < \alpha \ll 1$ the force (4.16) does not depend on the velocity and decreases with decreasing θ. The diffusion coefficient varies as

$$\bar{D} = \frac{\hbar^2k^2f^2\Gamma}{9(\delta^2+\Gamma^2/4)}\left(2 + \frac{9.54\delta^2\theta^2}{\Gamma^2\alpha^{1/3}}\right), \tag{4.17}$$

and decreases with decreasing θ and increasing velocity.

2. Large velocity, $\alpha \gg 1$

In the high-velocity limit, the force takes the form

$$\bar{F} = -\frac{\theta\hbar k f^2\delta\sin^2}{6\alpha(\delta^2+\Gamma^2/4)} = -\frac{\theta\hbar f^4\Gamma\delta\sin^2}{27v(\delta^2+\Gamma^2/4)^2}, \tag{4.18}$$

which is valid for any angle θ. The force (4.18) decreases with decreasing θ.

The diffusion coefficient is given by

$$\bar{D} = \frac{2\hbar^2k^2f^2\Gamma}{9(\delta^2+\Gamma^2/4)}\left[1 + \frac{\sin^2\theta}{16\alpha^2}\left(1 + \frac{18\delta^2}{\Gamma^2}\right)\right], \tag{4.19}$$

and decreases with decreasing θ and increasing velocity.

Results for the entire range of velocities are shown in Figs. 6 and 7. The velocity dependence of the force in the case of small angles θ differs dramatically from that obtained in the case $\theta = \pi/2$. For a given α the force $\bar{F}(\theta = \pi/2)$ is smaller than $\bar{F}(\pi/2 > \theta > \alpha^{1/2})$. An important new feature of the diffusion coefficient is the strong dependence of its sub-Doppler-limit part $D_{\rm ind}$ on angle θ. For $\theta = \pi/2$ and $|\delta| \gg \Gamma$ this part is the dominant one, as it is δ^2/Γ^2 times larger than the contribution $D_{\rm sp}$ brought about by the emission of spontaneous photons. However, $D_{\rm ind}$ decreases with decreasing θ, while $D_{\rm sp}$ does not vary significantly with θ. As a result, the diffusion coefficient D decreases with decreasing θ. Moreover, for a range of angles $\theta \ll 1$, one finds

$$D_{\rm ind} < D_{\rm sp} \tag{4.20}$$

even for small velocities.

B. Equilibrium momentum distribution

For $J_e = \frac{1}{2}$ and $\delta > 0$, the equilibrium momentum and spatial distribution $\psi_{\rm eq}(z,p)$ characterized by mean kinetic energy $E_{\rm eq} = p_{\rm eq}^2/(2M)$ results from the balance between the cooling force and diffusive heating. Rigorously, the equilibrium distribution is a solution of Eqs. (3.2) and (3.3); however, it may be possible to approximate this distribution using the Fokker-Planck equation (3.18) with a diffusion coefficient $\bar{D}(\theta,p)$ and a drift term $\bar{F}(\theta,p)$. The resulting distribution $\psi_{\rm eq}(p)$ is not necessarily of Gaussian form. Introducing a dimensionless atomic momentum

$$\beta = \frac{p}{\hbar k}, \tag{4.21}$$

and neglecting the dependence of $\bar{D}_{\rm sp}$ on velocity, one finds the distribution $\psi_{\rm eq}(\beta)$ to have the form

$$\psi_{\rm eq}(\beta) = \psi_{\rm eq}(0)\exp\left(-\hbar k\int_0^\beta \frac{\bar{F}}{\bar{D}}d\beta'\right). \tag{4.22}$$

Calculating the mean equilibrium kinetic energy $E_{\rm eq}$ as

$$E_{\rm eq} = E_R\int_{-\infty}^{\infty}\beta^2\psi_{\rm eq}(\beta)d\beta, \tag{4.23}$$

where $E_R = (\hbar k)^2/(2M)$ is the recoil energy, one arrives at the results presented in Figs. 8 and 9.

The mean kinetic energy as a function of dimensionless laser field intensity I defined by

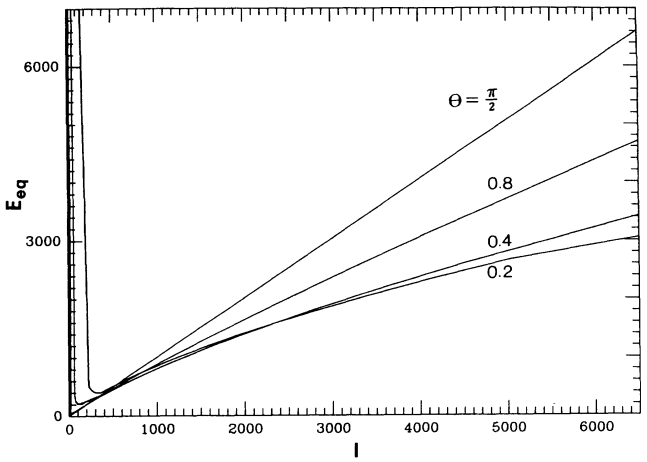

FIG. 8. Mean equilibrium kinetic energy E_{eq} in units of $\hbar^2k^2/2M$ (M is atomic mass) as a function of a dimensionless field intensity I defined by $I = |f|^2M/(3\hbar\delta k^2)$. The different curves correspond to different angles θ. The atom-field configuration is the same as that used to obtain Figs. 6 and 7.

$$I = U_0(\theta = 0, z = 0)/2E_R = \frac{f^2M}{3\hbar\delta k^2} \tag{4.24}$$

is shown in Fig. 8 for

$$\pi/2 \geq \theta \geq \Gamma/\delta. \tag{4.25}$$

Assuming that $|\delta| \gg \Gamma$, and using expressions for $\bar{F}$ and $\bar{D}$ in different velocity limits, one can get a qualitative understanding of the results presented in this figure. For $\theta = \pi/2$ one arrives at

$$\psi_{eq}(\beta) = \psi_{eq}(0)(1 + 2\beta^2/I^2)^{-I/4} \tag{4.26}$$

and

$$E_{eq} = E_R\frac{I^2}{I - 6}. \tag{4.27}$$

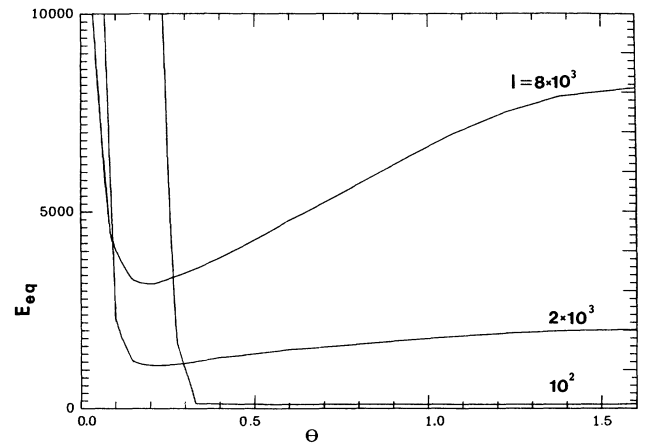

FIG. 9. Mean equilibrium kinetic energy E_{eq} in units of $\hbar^2k^2/2M$ (M is atomic mass) as a function of θ. The different curves correspond to a different dimensionless field intensity I defined by $I = |f|^2M/(3\hbar\delta k^2)$. The atom-field configuration is the same as that used to obtain Figs. 6 and 7.

If $\theta < \pi/2$, for relatively small intensity I satisfying the condition

$$\left(\frac{3\delta}{\Gamma}\right)^2 \gg I > 6\sin^{-2}\theta\ , \tag{4.28}$$

one has

$$\psi_{eq}(\beta) = \psi_{eq}(0)[1 + 2\beta^2/(I\sin\theta)^2]^{-I\sin^2\theta/4} \tag{4.29}$$

and

$$E_{eq} = E_R\frac{I^2\sin^2\theta}{I\sin^2\theta - 6}. \tag{4.30}$$

For $\theta \ll 1$ and I satisfying

$$\left(\frac{8\delta}{\Gamma\theta^2}\right)^2 \gg I \gg \left(\frac{3\delta}{\Gamma}\right)^2\ , \tag{4.31}$$

one arrives at

$$\psi_{eq} = \psi_{eq}(0)\exp\left[-0.3\left(\frac{\Gamma^2\beta^4}{\delta^2 I}\right)^{1/3}\right] \tag{4.32}$$

and

$$E_{eq} \approx E_R\frac{5.6\delta}{\Gamma}I^{1/2}. \tag{4.33}$$

For even higher intensities

$$I \gg \left(\frac{8\delta}{\Gamma\sin^2\theta}\right)^2\ , \tag{4.34}$$

the energy distribution takes the form

$$\psi_{eq} = \psi_{eq}(0)\exp(-\beta^2/2I\sin^2\theta), \tag{4.35}$$

and the mean kinetic energy is given by

$$E_{eq} = E_RI\sin^2\theta. \tag{4.36}$$

One can see from Fig. 8 that the minimal intensity that can still ensure an equilibrium energy distribution increases with θ as $6/\sin^2\theta$. The optimal cooling is obtained for $\theta = \frac{\pi}{2}$ and $I = 12$. However, for smaller θ and higher intensities, the mean kinetic energy as a function of I increases more slowly than for $\theta = \pi/2$, and in some angle range can be a decreasing function of θ. The dependence of E_{eq} on θ is shown in Fig. 9. For relatively low intensity satisfying

$$I < \left(\frac{8\delta}{\Gamma}\right)^2\ , \tag{4.37}$$

E_{eq} is given by Eqs. (4.30) and (4.33) and is almost insensitive to the angle unless it is very small. However, for higher intensity

$$\left(\frac{8\delta}{\Gamma}\right)^2 \ll I \ll \left(\frac{\delta}{\Gamma}\right)^{10} \tag{4.38}$$

and angles satisfying

$$\pi/2 > \theta \gg \left(\frac{64\delta^2}{\Gamma^2 I}\right)^{1/4}, \tag{4.39}$$

the equilibrium energy is given by Eq. (4.36) and varies as $\sin^2\theta$. If the angle gets even smaller, that is, if

$$\left(\frac{64\delta^2}{\Gamma^2 I}\right)^{1/4} \gg \theta \gg 0.5\left(\frac{\Gamma^6}{\delta^6 I}\right)^{1/8}, \tag{4.40}$$

$E_{\rm eq}$ is given by Eq. (4.33) and does not depend on θ. Finally, for very small angles

$$0.5\left(\frac{\Gamma^6}{\delta^6 I}\right)^{1/8} \gg \theta > \left(\frac{6}{I}\right)^{1/2}, \tag{4.41}$$

one has

$$E_{\rm eq} = E_R \frac{8I^2\Gamma^2}{9\delta^2(I\theta^2-4)(I\theta^2-6)} \tag{4.42}$$

and

$$\psi_{\rm eq}(\beta) = \psi_{\rm eq}(0)\left(1+\frac{3\delta\beta}{I\Gamma}\right)^{-I\theta^2/2}. \tag{4.43}$$

The mean kinetic energy (4.42) increases sharply with decreasing θ, and laser cooling is possible only for $\theta > (2/I)^{1/2}$.

One can see that the minimal equilibrium energy is achieved for a small angle θ satisfying the condition (4.40). From Eq. (4.33) one has

$$E_{\rm eq}^{\rm min} \approx E_{\rm eq}\left(\theta=\frac{\pi}{2}\right)\frac{5.6\delta}{\Gamma I^{1/2}}, \tag{4.44}$$

where

$$E_{\rm eq}\left(\theta=\frac{\pi}{2}\right) = \frac{\hbar f^2}{6\delta} \tag{4.45}$$

is the mean equilibrium energy reached for the laser beams with orthogonal polarizations. Taking into account Eq. (4.38) one can see that the energy $E_{\rm eq}^{\rm min}$ obtainable for small angles can be significantly smaller than $E_{\rm eq}(\theta=\frac{\pi}{2})$.

The results presented above for the equilibrium energy distribution have been derived using the Fokker-Planck equation (3.18) with the drift and diffusion coefficients averaged over the optical wavelength. However, one can deduce from Eq. (4.44) that, for small θ, the energy $E_{\rm eq}^{\rm min}$ is smaller than the maximum of the effective potential U_0. Consequently, an atom having this energy must be strongly localized [17]. This means that, rigorously speaking, the equilibrium energy distribution $\psi(z,p)$ should strongly depend on the center-of-mass position z, and that localization effects must play a significant role in the calculation of $E_{\rm eq}$. Although the results obtained using the averaged Fokker-Planck equation are quite similar for $J_e = 1/2$ and $3/2$ atoms, the localization effects make these two systems very different. It has been shown earlier that atomic motion in the vicinities of the laser field nodes is responsible for a dramatic increase of the frictional force and decrease of the sub-Doppler-limit momentum diffusion that may eventually lead to mean energies (4.44) and strong localization. For $J_e = 1/2$ the potential U_0 has its minima at the field nodes. Thus an atom trapped in a region

$$\delta z \sim \frac{1}{2k}\left(\frac{5.6\delta}{\Gamma I^{1/2}}\right)^{1/2}$$

near the field node may experience a very strong frictional force and may be cooled to the energies given by Eq.(4.44). However, the effective potential U_0 of the $J_e = 3/2$ atom has its minima at the antinodes of the laser standing wave. As soon as an atomic kinetic energy becomes smaller than $2U_0(z=0)$, an atom is trapped in the vicinity of the antinode where both the force and the sub-Doppler-limit diffusion coefficient are proportional to θ^2 and are small. As a result, one should have been expect to obtain weaker localization ($\delta z \sim \pi/6k$) and the equilibrium kinetic energy of order $E_{\rm eq}(\theta=\pi/2)$ for a wide range of angles θ .

V. CONCLUSIONS

We have seen that in the one-dimensional field configuration with almost parallel linear polarizations of the counterpropagating laser beams the considerable increase of the effective optical relaxation time and the population difference gradient near the nodes of the field may lead to significant cooling and localization of the atomic particles having $J_g = \frac{1}{2}$. Identical effects would occur if the linearly polarized fields were replaced by two circularly polarized standing-wave fields (polarizations $\mathbf{e}_+$ and $\mathbf{e}_-$, relative phase shift $\theta \ll 1$). Although the calculation has been limited to the $J_g = \frac{1}{2}$ ground state, one would expect a similar qualitative behavior for other values of J_g. To account for the rapid spatial variation of the ground-state population difference, new analytical approaches are needed since methods based on Fourier series or expansions about $v = 0$ may converge very slowly. The need for new analytical techniques is underscored if the results are generalized to two-dimensional cooling. In this case, for certain field configurations, we find a dependence of the friction force which varies as $F_{x,y} \sim \alpha_{x,y}\ln(\alpha_x^2+\alpha_y^2)$, where $\alpha_{x,y} = kv_{x,y}\tau_p$.

As an example of a method by which one can measure directly the dependence of the spatially averaged cooling force on angle θ, we should like to cite the recent experiment of Grynberg, Vallet, and Pinard [18]. They measured the changes in field intensity as two copropagating waves traverse a medium of $J = \frac{1}{2}$ ground-state atoms as a function of the frequency difference δ' between the waves. The changes in field intensity can be related directly to the spatially averaged friction force that would appear in the sub-Doppler-limit laser cooling. The two fields they used were linearly polarized with an angle $\theta = \pi/2$. The characteristic width they found in their experiment is consistent with the capture range that would appear in the sub-Doppler-limit laser cooling. In the similar type of measurement, by changing angle θ between the field polarization directions one might see the increase of the signal gradient about $\delta' = 0$ corresponding to the increase of the cooling force for small angles found in this paper.

ACKNOWLEDGMENTS

This research is supported by the U.S. Office of Naval Research and the National Science Foundation Grants Nos. PHY-8814423 and INT-8815306.

APPENDIX: DERIVATION OF EQS. (3.2) AND (3.3)

In this paper we consider atoms having ground and excited-state angular momenta $J_g = \frac{1}{2}$ and $J_e = \frac{1}{2}$ or $\frac{3}{2}$. The atomic density matrix satisfies the equation

$$\frac{d\rho}{dt} = \frac{i}{\hbar}[\rho, H] + \mathrm{Rel}(\rho), \tag{A1}$$

where the Hamiltonian H is given by

$$H = \frac{p^2}{2M} + H_{\mathrm{at}} + H_{\mathrm{af}}, \tag{A2}$$

with $p = Mv$ and M denoting the atomic momentum and mass, respectively. In the rotating-wave approximation, the atomic Hamiltonian H_{at} is given by

$$H_{\mathrm{at}} = -\hbar\delta \sum_{m_e=-J_e}^{J_e} |J_e, m_e\rangle\langle J_e, m_e|. \tag{A3}$$

For $J_e = \frac{1}{2}$, the interaction part of the Hamiltonian H_{af}, which describes atom-field coupling, has the form

$$H_{\mathrm{af}} = \hbar f\sqrt{\frac{2}{3}}\left[\cos\left(\frac{\theta}{2} + kz\right)|e_{1/2}\rangle\langle g_{-1/2}| - \cos\left(-\frac{\theta}{2} + kz\right)|e_{-1/2}\rangle\langle g_{1/2}|\right], \tag{A4}$$

where z is the atomic center-of-mass position. In the case $J_e = \frac{3}{2}$ one has

$$H_{\mathrm{af}} = \frac{\hbar f}{\sqrt{2}}\left[\cos\left(\frac{\theta}{2} + kz\right)\left(|e_{3/2}\rangle\langle g_{1/2}| + \frac{1}{\sqrt{3}}|e_{1/2}\rangle\langle g_{-1/2}|\right) - \cos\left(-\frac{\theta}{2} + kz\right)\left(|e_{-3/2}\rangle\langle g_{-1/2}| + \frac{1}{\sqrt{3}}|e_{-1/2}\rangle\langle g_{1/2}|\right)\right]. \tag{A5}$$

The relaxation due to spontaneous-emission processes is included in the term $\mathrm{Rel}(\rho)$.

Using the weak-field condition (1.1) one can adiabatically eliminate the excited-state populations and excited-ground-state coherences [4]. For the density matrix in the Wigner representation defined by

$$\rho(z,p) = (2\pi\hbar)^{-1}\int \rho(p + \tfrac{1}{2}q, p - \tfrac{1}{2}q)e^{iqz/\hbar}dq, \tag{A6}$$

in the $J_e = \frac{1}{2}$ case, one finds the quasistationary solution

$$\rho_{e\pm1/2\ g\mp1/2}(p,z) \approx \pm\frac{1}{\sqrt{6}}\frac{f}{(\delta + i\Gamma/2)}[\rho_{g\mp1/2\ g\mp1/2}(p - \tfrac{1}{2}\hbar k, z)e^{i(\pm\frac{1}{2}\theta + kz)} + \rho_{g\mp1/2\ g\mp1/2}(p + \tfrac{1}{2}\hbar k, z)e^{-i(\pm\frac{1}{2}\theta + kz)}] \tag{A7}$$

and

$$\rho_{e\pm1/2\ e\pm1/2}(p,z) \approx i\frac{1}{6}\frac{f^2}{\Gamma(\delta^2 + \Gamma^2/4)}[2\rho_{g\mp1/2\ g\mp1/2}(p,z)\cos(\pm\theta + 2kz) + \rho_{g\mp1/2\ g\mp1/2}(p + \hbar k, z) + \rho_{g\mp1/2\ g\mp1/2}(p - \hbar k, z)] + \mathrm{c.c.} \tag{A8}$$

The ground-state populations evolve as

$$\frac{d}{dt}\rho_{g\pm1/2\ g\pm1/2}(p,z) = \pm\frac{if}{\sqrt{6}}[\rho_{e\mp1/2\ g\pm1/2}(p - \tfrac{1}{2}\hbar k, z)e^{i(\mp\frac{1}{2}\theta + kz)} + \rho_{e\mp1/2\ g\pm1/2}(p + \tfrac{1}{2}\hbar k, z)e^{-i(\mp\frac{1}{2}\theta + kz)}] \pm \mathrm{c.c.} + \frac{1}{2}\Gamma\int_{-1}^{1}[(1+q^2)\rho_{e\mp1/2\ e\mp1/2}(p + \hbar kq, z) + (1-q^2)\rho_{e\pm1/2\ e\pm1/2}(p + \hbar kq, z)]dq, \tag{A9}$$

where the integral term accounts for the repopulation of those levels resulting from the emission of circularly and linearly polarized photons from the excited state [14]. Substituting Eqs. (A7) and (A8) into Eq. (A9) for the ground-state sublevel populations, one arrives at the closed set of equations

$$\frac{d}{dt}\rho_{\pm}(p,z) = -\frac{\Gamma f^2}{6(\delta^2+\Gamma^2/4)}\left(2\rho_{\pm}(p,z) + \cos(\mp\theta+2kz)[\rho_{\pm}(p+\hbar k,z)+\rho_{\pm}(p-\hbar k,z)] + \frac{2\delta}{\Gamma}\sin(\mp\theta+2kz)[\rho_{\pm}(p+\hbar k,z)-\rho_{\pm}(p-\hbar k,z)]\right)$$
$$+\frac{\Gamma f^2}{24(\delta^2+\Gamma^2/4)}\int_{-1}^{1}\{(1+q^2)[\rho_{\pm}(p+\hbar k(q+1),z)+\rho_{\pm}(p+\hbar k(q-1),z) +2\rho_{\pm}(p+\hbar kq,z)\cos(\mp\theta+2kz)] + (1-q^2)[\rho_{\mp}(p+\hbar k(q+1),z) +\rho_{\mp}(p+\hbar k(q-1),z)+2\rho_{\mp}(p+\hbar kq,z)\cos(\pm\theta+2kz)]\}dq, \tag{A10}$$

where $\rho_{\pm} = \rho_{g\pm 1/2\, g\pm 1/2}$.

For an atom having $J_e = \frac{3}{2}$ the corresponding equations are

$$\frac{d}{dt}\rho_{\pm}(p,z) = -\frac{\Gamma f^2}{24(\delta^2+\Gamma^2/4)}\left(8\rho_{\pm}(p,z) + [3\cos(\pm\theta+2kz)+\cos(\mp\theta+2kz)][\rho_{\pm}(p+\hbar k,z)+\rho_{\pm}(p-\hbar k,z)] + \frac{2\delta}{\Gamma}[3\sin(\pm\theta+2kz)+\sin(\mp\theta+2kz)][\rho_{\pm}(p+\hbar k,z)-\rho_{\pm}(p-\hbar k,z)]\right)$$
$$+\frac{\Gamma f^2}{96(\delta^2+\Gamma^2/4)}\int_{-1}^{1}\{(1+q^2)\{5\rho_{\pm}(p+\hbar k(q+1),z)+5\rho_{\pm}(p+\hbar k(q-1),z) +\rho_{\pm}(p+\hbar kq,x)[9\cos(\pm\theta+2kz)+\cos(\mp\theta+2kz)]\} +2(1-q^2)[\rho_{\mp}(p+\hbar k(q+1),z)+\rho_{\mp}(p+\hbar k(q-1),z) +2\rho_{\mp}(p+\hbar kq,z)\cos(\pm\theta+2kz)]\}dq. \tag{A11}$$

Equations (A10) and (A11) are exact under the weak-field assumption (1.1). If, in addition, one assumes that an atomic momentum is much larger than that of the photon, that is

$$p \gg \hbar k, \tag{A12}$$

one can expand these equations to second order in $\hbar k$ to arrive at Eqs. (3.2) and (3.3) for $J_e = \frac{1}{2}$ and $\frac{3}{2}$, respectively.

[1] J. Dalibard and C. Cohen-Tannoudji, J. Opt. Soc. Am. B **6**, 2023 (1989).

[2] P. Ungar, D. Weiss, E. Riis, and S. Chu, J. Opt. Soc. Am. B **6**, 2058 (1989).

[3] A. Aspect, E. Arimondo, R. Kaiser, N. Vanteenkiste, and C. Cohen-Tannoudji, J. Opt. Soc. Am. B **6**, 2112 (1989).

[4] Y. Castin, J. Dalibard, and C. Cohen-Tannoudji, in *Light Induced Kinetic Effects of Atoms and Molecules*, edited by L. Moi, S. Gozzini, C. Gabbannini, E. Arimondo, and F. Strumia (Ets Editrice, Pisa, 1991), p. 5.

[5] J. Shevy, Phys. Rev. A **41**, 5229 (1990).

[6] P. Berman, Phys. Rev. A **43**, 1470 (1991).

[7] G. Nienhuis, P. van der Straten, and S.-Q. Shang, Phys. Rev. A **44**, 462 (1991).

[8] P. Lett, R. Watts, C. Westbrook, W. Phillips, P. Gould, and H. Metcalf, Phys. Rev Lett. **61**, 169 (1988).

[9] P. Lett, W. Phillips, S. Rolston, C. Tanner, R. Watts, and C. Westbrook, J. Opt. Soc. Am. B **6**, 2084 (1989).

[10] D. Weiss, E. Riis, Y. Shevy, P. Ungar, and S. Chu, J. Opt. Soc. Am. B **6**, 2072 (1989).

[11] C. Solomon, J. Dalibard, W. Phillips, A. Clairon, and S. Guellati, Europhys. Lett. **12**, 683 (1990).

[12] B. Sheehy, S.-Q. Shang, R. Watts, S. Hatamian, and H. Metcalf, J. Opt. Soc. Am. B **6**, 2165 (1989).

[13] As shown in [4], owing to decrease of the momentum diffusion coefficient for large atomic velocities, an actual capture range is much wider and is not restricted by condition (2.24).

[14] V. S. Letokhov and V. G. Minogin, Phys. Rep. **73**, 1 (1981).

[15] It can be shown that more accurate calculation leads to some correction for the momentum diffusion coefficient in the limit of very small velocities $kv\tau_p \ll \theta^3$. As the high-precision calculation of the minimal achievable atomic kinetic energy is not the goal of this article, here we do not take into account this correction.

[16] *Handbook of Mathematical Functions*, edited by M. Abramowitz and I.A. Stegun (Dover, New York, 1970).

[17] Since the amplitude of an effective laser-field potential is four times larger for a small angle θ than for $\theta = \pi/2$ [see Eq. (4.9)], one might expect to get much better localization of cooled atoms for $\theta \ll 1$ than for $\theta = \frac{\pi}{2}$, even when $E_{\rm eq}(\theta \ll 1) \approx E_{\rm eq}(\theta = \pi/2)$.

[18] G. Grynberg, M. Vallet, and M. Pinard, Phys. Rev. Lett. **65**, 701 (1990).